TECHNICAL UNIVERSITY OF CLUJ-NAPOCA

ACTA TECHNICA NAPOCENSIS

Series: Applied Mathematics, Mechanics, and Engineering
Vol. 63, Issue III, September, 2020

DESIGN OF AN INSPECTION ROBOT BASED ON THE PANTOGRAPH MECHANISM

Călin RUSU, Mihai Olimpiu TĂTAR

Abstract: *To move inside pipelines inspection robots must be able to adapt to geometric changes of pipes. This paper presents the design of a simple pipe inspection robot whose structure is based on a pantograph mechanism. Thus, at the beginning of the paper is presented a short classification of robots in the pipeline, followed by the determination of the expressions of reaction forces and traction force. In the last part, the proposed inspection robot is described.*
Key words: *in-pipe robots, adaptable structure, wheel-based locomotion*

1. INTRODUCTION

There is a wide variety of pipe networks that need to be inspected and whose safety and integrity must be guaranteed. A large majority of this pipelines can be easily inspected using the so-called Pipeline Inspection Gauges or PIGs. These devices do not have a propulsion system and are driven by the transported fluid. Thus, PIGs are uncontrollable and unable to adapt to changes in pipe direction or diameter [1].

Inspection of fluid-free pipelines or which have sudden changes of direction, involves the use of robots. In-pipe inspection has many challenges, mainly due to limited workspace to which robots must adapt.

A major challenge is to ensure the traction within the environment. The most relevant methods used for this purpose are presented in [1]. These are based on: gravity, wall-pressing, adhesion and fluid-flow. Wall-pressing is the most widely used method for ensuring traction inside the pipe. Various types locomotion is also possible: wheel-based, caterpillar-type, walking, helical, peristaltic or snake-type [1], [2]. Several examples of wall-pressed robots with hybrid locomotion systems are reviewed in [3]. Wall-pressing robots usually use one or more parallelogram or pantograph scissor mechanisms to remain centered inside the pipe. Until now, many researches have been focused on the design and development of wall-pressing in-pipe inspection robots.

The MOGRER robot presented in paper [4] is among the first wall-pressing devices. It uses springs and a planar pantograph mechanism to adapt itself to changes in pipe diameter. Robots based on planar mechanisms face a stability problem. Any loss of contact with pipe walls will decentralize the robot. In paper [5] is presented an inspection robot that is in contact with the pipe wall in three planes arranged at 120^0. Inspection robots also must develop enough traction force to pull their cables and equipment. In paper [6] are presented details regarding the design of three mini-robots with adaptable structure for in-pipe inspection and the experimental determination of their traction force. In order to perform their tasks, in-pipe robots can be equipped with various auxiliary devices, including robotic arms. Such an example is presented in paper [7].

2. STRUCTURE OF THE INSPECTION ROBOT

The in-pipe inspection robot proposed in this paper is based on the prototype developed in [8] This inspection robot belongs to the category of wall pressing robots that are in contact with the pipe in a single plane. Its schematic structure is shown in Figure 1.

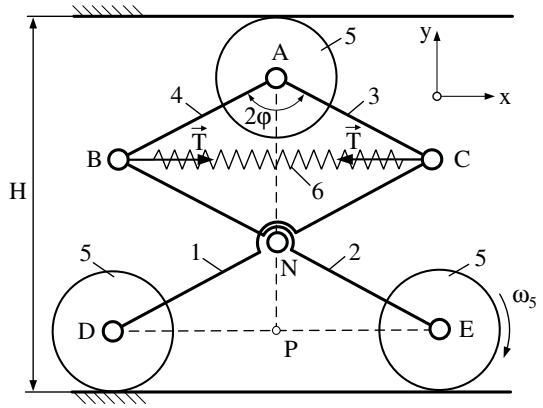

Fig. 1. Schematic structure of wall-pressing robot

Its structure is based on a pantograph mechanism, consisting of elements marked with 1,2,3 and 4 respectively. In the joints denoted with A, D and E are placed three wheels (5) that ensure the contact with the inner surface of the pipe. At least one of these wheels is driven by an electric motor and make possible the movement of the robot inside the pipe. The contact between the wheels and the pipe is maintained due to the force $\vec{T}$ developed by one or more helical springs (6) placed between joints *B* and *C*.

Like other robots in the same category, the proposed robot uses the pantograph mechanism to adapt to diameter change of the pipe. Thus, the robot was designed to inspect pipes with diameters between 80 and 110 mm. In order to achieve this goal, the mechanism's elements have the following lengths: AB = AC = l_1= 36 mm, BE = CD = l_2= 72 mm, and radius of wheels is r =15 mm.

The movement of the robot is greatly influenced by the shape, diameter and curvature of the pipe. Due to the action of the helical spring, the structure of the robot tends to minimize the value of angle denoted with φ in Figure1. From a geometric point of view, the height *H* of the robot structure and the inner diameter of the pipe must be equal. In this case all wheels will be in contact with the pipe in its maximum longitudinal section. The height of the robot is given by:

$$H = 2r + l_1 \cos\varphi + l_2 \cos\varphi \qquad (1)$$

Next, the reaction forces between the wheels and the pipe and the expression of the traction force to be generated by the drive wheel, will be determined.

3. STATIC FORCE ANALISYS

The reaction forces between the wheels and the pipe wall were determined using the method proposed by the authors of paper [4].

Thus, it was considered for the robot a simplified T-shaped plane structure presented in Figure 2, in which DE = $2l_x$ and AP = l_y. The vertical part of the T-shaped structure can extend and retract generating a force $\vec{F}$ which will act upon the surface of the pipe wall.

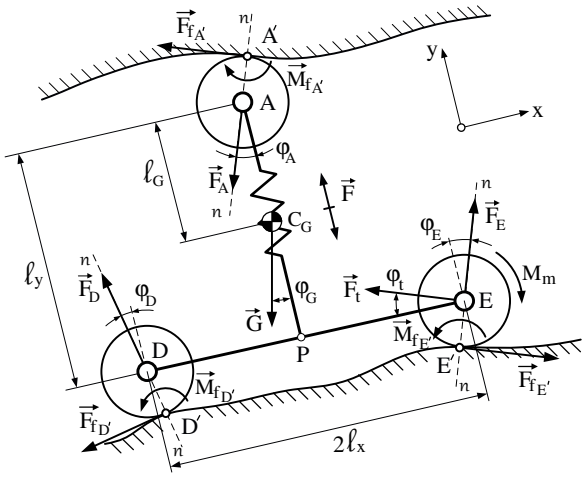

Fig. 2. Simplified structure used for static force analysis

All three wheels are in contact with the pipe wall at the points *A'*, *D'* and *E'*. With $\vec{F}_A$, $\vec{F}_D$ and $\vec{F}_E$ are denoted the reaction forces which appear between the pipe and the wheels. These reactions are normal in the points of contact between the pipe wall and wheels and pass through the center of joints *A*, *D*, and *E*.

φ_A, φ_D and φ_E are the angles between the reaction forces and axes parallel to Oy. The angle between the traction force $\vec{F}_t$ and Ox is denoted with φ_t ($\varphi_t = \varphi_E$) and φ_G is the inclination angle of the pipe.

We assuming that the gravity center is located in C_G, at a distance l_G measured from the center of joint *A*. With $\vec{G}$ we denote the weight of the robot, which includes mechanism's elements, wheels, motors, springs etc.

Figure 2 also shows the friction forces $\vec{F}_{fA'}, \vec{F}_{fD'} \vec{F}_{fE'}$ and moments $\vec{M}_{fA'}, \vec{M}_{fD'}, \vec{M}_{fE'}$ between the wheels and pipe wall.

Forces projections equations can be written as follows:

$$\begin{cases} -F_A \sin\varphi_A - F_D \sin\varphi_D + F_E \sin\varphi_E - \\ \quad -G \sin\varphi_G - F_t \cos\varphi_E = 0 \\ -F_A \cos\varphi_A + F_D \cos\varphi_D + F_E \cos\varphi_E - \\ \quad -G \cos\varphi_G + F_t \sin\varphi_E = 0 \end{cases} \quad (2)$$

The sum of moments with respect to point *A* is:

$$\begin{aligned} F_E \cos\varphi_E\, l_x + F_E \sin\varphi_E\, l_y - F_D \cos\varphi_D\, l_x - \\ -F_D \sin\varphi_D\, l_y - G l_G \sin\varphi_G + \\ +F_t \sin\varphi_E\, l_x - F_t \cos\varphi_E\, l_y = 0 \end{aligned} \quad (3)$$

Static force balance in point *A* yields:

$$F_A \cos\varphi_A = F - \left(1 - \frac{l_G}{l_y}\right) G \cos\varphi_G \quad (4)$$

Thus, the resulting equations system can be written as follows:

$$\begin{cases} -F_D \sin\varphi_D + F_E \sin\varphi_E - F_t \cos\varphi_E = \\ \quad = G \sin\varphi_G + F_A \sin\varphi_A \\ F_D \cos\varphi_D + F_E \cos\varphi_E + F_t \sin\varphi_E = \\ \quad = G \cos\varphi_G + F_A \cos\varphi_A \\ F_D(-l_x \cos\varphi_D - l_y \sin\varphi_D) + \\ \quad +F_E(l_x \cos\varphi_E + l_y \sin\varphi_E) + \\ \quad +F_t(l_x \sin\varphi_E - l_y \cos\varphi_E) = \\ \quad = G l_G \sin\theta_G \end{cases} \quad (5)$$

The expression of reaction force F_A can be easily obtained from equation 4:

$$F_A = \frac{1}{\cos\varphi_A}\left[F - \left(1 - \frac{l_G}{l_y}\right) G \cos\varphi_G\right] \quad (6)$$

In order to determine the remaining forces, the system (5) must be solved. Thus, it results:

$$F_D = \frac{\begin{vmatrix} a_{11} & a_{12} & a_{13} \\ a_{21} & a_{22} & a_{23} \\ a_{31} & a_{32} & a_{33} \end{vmatrix}}{\begin{vmatrix} b_{11} & b_{12} & b_{13} \\ b_{21} & b_{22} & b_{23} \\ b_{31} & b_{32} & b_{33} \end{vmatrix}} \quad (7)$$

$$F_E = \frac{\begin{vmatrix} c_{11} & c_{12} & c_{13} \\ c_{21} & c_{22} & c_{23} \\ c_{31} & c_{32} & c_{33} \end{vmatrix}}{\begin{vmatrix} b_{11} & b_{12} & b_{13} \\ b_{21} & b_{22} & b_{23} \\ b_{31} & b_{32} & b_{33} \end{vmatrix}} \quad (8)$$

$$F_t = \frac{\begin{vmatrix} d_{11} & d_{12} & d_{13} \\ d_{21} & d_{22} & d_{23} \\ d_{31} & d_{32} & d_{33} \end{vmatrix}}{\begin{vmatrix} b_{11} & b_{12} & b_{13} \\ b_{21} & b_{22} & b_{23} \\ b_{31} & b_{32} & b_{33} \end{vmatrix}} \quad (9)$$

where:

$$\begin{aligned} &a_{11} = c_{12} = d_{13} = \\ &= G \sin\varphi_G + tg\varphi_A \left[F - \left(1 - \frac{l_G}{l_y}\right) G \cos\varphi_G\right] \\ &a_{12} = a_{23} = b_{12} = b_{23} = c_{23} = d_{12} = \sin\varphi_E \\ &a_{13} = b_{13} = c_{13} = -\cos\varphi_E \\ &a_{21} = c_{22} = d_{23} = G \cos\varphi_G \left[F + \frac{l_G}{l_y}\right] \\ &a_{22} = b_{22} = d_{22} = \cos\varphi_E \\ &a_{31} = c_{32} = d_{33} = G \sin\varphi_G\, l_G \\ &a_{32} = b_{32} = d_{32} = l_y \sin\varphi_E + l_x \cos\varphi_E \\ &a_{33} = b_{33} = c_{33} = l_x \sin\varphi_E - l_y \cos\varphi_E \\ &b_{11} = c_{11} = d_{11} = -\sin\varphi_D \\ &b_{21} = c_{21} = d_{21} = \cos\varphi_D \\ &b_{31} = c_{31} = d_{31} = -(l_x \cos\varphi_D + l_y \sin\varphi_D) \end{aligned} \quad (10)$$

The force F can be expressed as a function of the spring tension $\vec{T}$ and angle φ, as follows:

$$F = 4 l_2 k (\sin\varphi - \sin\varphi_{min}) ctg(\varphi) \quad (11)$$

where: k is the spring constant and φ_{min} represents the value of the angle for the maximum height of the robot (H = 110mm).

If we consider the simplifying hypothesis in which $\varphi_A = \varphi_D = \varphi_E = 0$, it will be possible to calculate the values of the reactions and the traction force, for different values of the angle φ_G. The necessary condition so that there is no slip between the drive wheel and the pipe wall, can be written as:

$$\mu F_E \geq F_t \quad (12)$$

Therefore, the torque required for the drive wheel to roll without slipping into the pipe, is:

$$M_m \geq s F_E + F_t r \quad (13)$$

where: μ and *s* represents the friction and rolling coefficients.

4. THE PROPOSED DESIGN

Figure 3 shows the 3D model of proposed robot. Its structure is based on the pantograph mechanism formed by the symmetrical elements 1 and 2. In the marginal joints are placed three wheels denoted with 3, with a radius r = 30 mm and a width b = 9 mm. One of these wheels is driven by a 6 V miniature DC motor (4) with a right-angle gearbox. The wall pressing force is ensured by a helical spring (5).

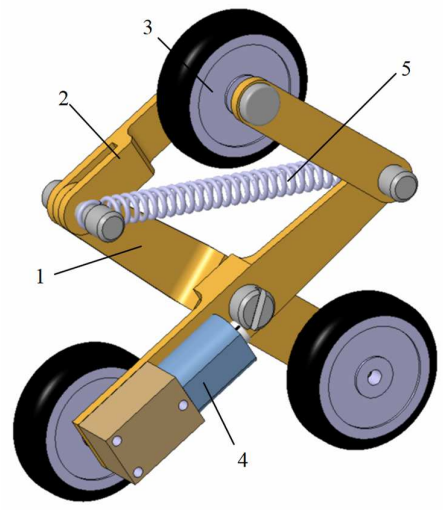

Fig.3. CAD model of proposed robot

An inspection video camera can be attached to this basic structure, using auxiliary elements.

5. CONCLUSION

The paper presented the main aspects related to the design of a robot for pipeline inspection. Optimizing the proposed structure to improve stability and increase the number of drive wheels to generate a high traction force are the main developments that authors intends to achieve.

6. REFERENCES

[1] Mills, G.H., Jackson, A.E., Richardson, R.C., *Advances in the Inspection of Unpiggable Pipelines* in Robotics Vol 6, nr 4, 2017.

[2] Decai, Z., Heping, C., Dong, W., Wangzhe, S., Dewei, M., Xiaoli, H., Siwen, F., *Design and Analysis of Drive Mechanism of Piping Robot*, Journal of Robotics and Automation, vol 3, no 1, pp.106-111, 2019.

[3] Roslin, N., Anuar, A., Abdul Jalal, M.F., Sahari, K., *A Review: Hybrid Locomotion of In-pipe Inspection Robot* in Procedia Engineering vol 41, pp.1456-1462, 2012.

[4] Okada, T., Sanemori, T., *MOGRER: A vehicle study and realization for in-pipe inspection tasks*, in IEEE Journal on Robotics and Automation, vol. 3, no. 6, pp. 573-582, 1987.

[5] Tătar, M.O., Cirebea, C., Aluţei, A., Mândru, D., *The Design of Adaptable Indoor Pipeline Inspection Robots*, Proceedings of the 2012 IEEE International Conference on Automation, Quality and Testing, Robotics (AQTR) Theta 18, pp, 443-448, Cluj-Napoca, Romania, 2012

[6] Tatar, M.O, Ardelean, I., Mandru, D., *Adaptable Robots Based on Linkage Type Mechanisms for Pipeline Inspection Task*, in Applied Mechanics and Materials, Vol 762, pp.163-168. 2015.

[7] Lapusan, C., Rusu, C., Brai, L., Mandru, D., *Development of a multifunctional robotic arm for in-pipe robots*, 7th International Conference on Electronics, Computers and Artificial Intelligence (ECAI), Bucharest, pp. WR-11-WR-14, 2015

[8] PNII - IDEI Project, ID_1056: *Modelling, simulation and development of robotic system families used for inspection and exploration*.

PROIECTAREA UNUI ROBOT DE INSPECTIE BAZAT PE MECANISMUL PANTOGRAF

Rezumat: Pentru a se deplasa în interiorul conductelor, roboții de inspecție trebuie să se poată adapta la modificările geometrice ale acestora. Această lucrare prezintă proiectarea unui robot simplu de inspecție în țevi a cărui structură se bazează pe un mecanism de pantograf. Astfel, la începutul lucrării este prezentată o scurtă clasificare a roboților de inspectie, urmată de determinarea expresiilor reacțiunilor și a forței de tracțiune. În ultima parte, este descris robotul de inspecție propus

Călin RUSU, PhD.Eng., Lecturer, Technical University of Cluj-Napoca, Department of Mechatronics and Machine Dynamics, calin.rusu@mdm.utcluj.ro

Mihai Olimpiu TĂTAR, PhD.Eng., Professor, Technical University of Cluj-Napoca, Department of Mechatronics and Machine Dynamics, olimpiu.tatar@mdm.utcluj.ro